Theoretical study of molecular hydrogen and spiltover hydrogen storage on two-dimensional covalent-organic frameworks*

Liu Xiu-Ying(刘秀英)[a)†], He Jie(何 杰)[a)], Yu Jing-Xin(于景新)[a)],
Li Zheng-Xin(栗正新)[b)], and Fan Zhi-Qin(樊志琴)[a)]

[a)] College of Science, Henan University of Technology, Zhengzhou 450000, China
[b)] School of Material Science and Engineering, Henan University of Technology, Zhengzhou 450000, China

(Received 22 September 2013; revised manuscript received 18 December 2013; published online 10 April 2014)

Molecular hydrogen and spiltover hydrogen storages on five two-dimensional (2D) covalent-organic frameworks (COFs) (PPy-COF, TP-COF, BTP-COF, COF-18 Å, and HHTP-DPB COF) are investigated using the grand canonical Monte Carlo (GCMC) simulations and the density functional theory (DFT), respectively. The GCMC simulated results show that HHTP-DPB COF has the best performance for hydrogen storage, followed by BTP-COF, TP-COF, COF-18 Å, and PPy-COF. However, their adsorption amounts at room temperature are all too low to meet the uptake target set by US Department of Energy (US-DOE) and enable practical applications. The effects of pore size, surface area, and isosteric heat of hydrogen on adsorption amount are considered, which indicate that these three factors are all the important factors for determining the H_2 adsorption amount. The chemisorptions of spiltover hydrogen atoms on these five COFs represented by the cluster models are investigated using the DFT method. The saturation cluster models are constructed by considering all possible adsorption sites for these cluster models. The average binding energy of a hydrogen atom and the saturation hydrogen storage density are calculated. The large average binding energy indicates that the spillover process may proceed smoothly and reversibly. The saturation hydrogen storage density is much larger than the physisorption uptake of H_2 molecules at 298 K and 100 bar (1 bar = 10^5 Pa), and is close to or exceeds the 2010 US-DOE target of 6 wt% for hydrogen storage. This suggests that the hydrogen storage capacities of these COFs by spillover may be significantly enhanced. Thus 2D COFs studied in this paper are suitable hydrogen storage media by spillover.

Keywords: hydrogen spillover, covalent-organic frameworks, hydrogen storage, grand canonical Monte Carlo simulation

PACS: 73.22.–f, 36.40.–c, 71.15.Mb **DOI:** 10.1088/1674-1056/23/6/067303

1. Introduction

Hydrogen storage is widely recognized as a critical enabling technology for the successful commercialization and market acceptance of hydrogen-powered vehicles. However, storing sufficient hydrogen on-board a wide range of vehicle platforms is a tremendous technical challenge. The US Department of Energy (US-DOE) has established the hydrogen storage targets of 6 wt% (9 wt%) and 45 g/L (81 g/L) for the year 2010 (2015).[1] In order to achieve this target, many scientific groups are devoting their efforts to the investigation of new storage techniques and methods, mainly including cryogenic liquid, pressurized gas, organic compound, metal hydrides, and porous materials. However, none of these methods completely satisfy all the criteria for the amount of hydrogen that can be supplied from a given weight or volume of tank for transport purposes.

In the recent developments of porous materials, covalent-organic frameworks (COFs) have received great attention both in synthesis and in the technological applications.[2–10] COFs are entirely constructed from light elements (B, C, O, N, and Si) that are linked by strong covalent bonds (B–C, B–O, C–C, C–N, and C–Si) to make a highly porous class of materials. They have the advantages of good stability, large surface area, porosity and extremely low density that could be suitable for gas storage. Therefore, a large number of experimental and theoretical studies of hydrogen storage on COFs materials have been reported since COFs were first synthesized in 2005.[2] Recent studies showed that COFs exhibit promising hydrogen storage capacities at very low temperatures.[3–10] For example, the hydrogen uptake of COF-108 reaches 21 wt% at 77 K and 100 bar.[8] However, their hydrogen storage capacity is not satisfactory at room temperature, which is too low to meet the uptake target set by US-DOE and enable practical applications. This is attributed to the very weak van der Waals (VDW) interactions between H_2 and COFs (about 2 kJ/mol–5 kJ/mol).[9] The binding energies of hydrogen storage systems in moderate conditions (−30 °C–80 °C and 1 bar–100 bar) should be 9.6 kJ/mol–58 kJ/mol.[11]

In order to enhance the hydrogen storage capacities of COFs at room temperature, many approaches have been proposed and conducted, both experimentally and theoretically.[12–20] The hydrogen adsorption via spillover

*Project supported by the National Natural Science Foundation of China (Grant Nos. 11247275 and 11304079), the Young Core Instructor of the Higher Education Institutions of Henan Province, the Special Foundation for Fostering Technologic Innovative Talents of Henan University of Technology, China (Grant No. 2012CXRC16), and the Natural Science Foundation of Education Bureau of Henan Province, China (Grant Nos. 2011B140005 and 13A140195).

†Corresponding author. E-mail: liuxiuyingzx@126.com

© 2014 Chinese Physical Society and IOP Publishing Ltd

is one of the most promising approaches,[20–24] which has been experimentally demonstrated by using a number of sorbents, including activated carbons,[21] carbon nanotubes,[21] graphite nanofibers,[22] zeolites,[23] metal–organic frameworks (MOFs),[20,24] and covalent-organic frameworks (COFs).[20] Hydrogen spillover is defined as the dissociative chemisorption of hydrogen molecules on metal nanoparticles, and subsequent migration of hydrogen atoms onto adjacent surfaces of a receptor via spillover and surface diffusion.[21] Because the binding of a spiltover hydrogen atom and the receptor surface is much stronger than that in the physical adsorption system, where the hydrogen molecule is adsorbed by the weak VDW interaction,[25,26] the hydrogen uptake by spillover in porous materials can be enhanced substantially. For example, Li and Yang[20] have done pioneering work on hydrogen spillover in MOFs. They mixed a small quantity of supported Pt catalyst (Pt/AC) with IRMOF-1 and with IRMOF-8 and used carbonated sugar to provide better contact between the materials. They found that the hydrogen uptakes increased to 3 wt% for IRMOF-1 and 4 wt% for IRMOF-8 at 298 K and 100 bar. In 2008, they studied the effect of hydrogen spillover on the storage capacity of metal–organic frameworks (MIL-101 and HKUST-1) and covalent-organic frameworks (COF-1).[24] They have demonstrated that the hydrogen adsorption capacity by bridged spillover could be enhanced by a factor of 2.6–3.2. This is the first time that the hydrogen storage capacity of COFs by spillover has been investigated experimentally. Theoretically, Suri *et al.*[18] and Ganz and Dornfeld[19] used *ab initio* quantum chemistry calculation to study the hydrogen storage capacities of several MOFs and COFs (COF-1 and COF-5) by spillover in 2009 and 2012, respectively. They predicted the saturation storage capacity by constructing saturation models, and found that the current experimental hydrogen uptakes of a majority of MOFs were not optimized and could be dramatically improved. However, only the hydrogen storage capacities of COF-1 and COF-5 by spillover have been studied. Experimentally, the structures of many COF materials are quite complex and the experimental condition is difficult to control, thus the number of COFs that have been synthesized is very limited. Furthermore, the sample preparation for these hydrogen spillover experiments is also very difficult. Therefore, it is necessary to study the hydrogen storage properties of COFs by spillover theoretically.

Based on the above and other reasons, we consider five 2D COFs (PPy-COF, BTP-COF, TP-COF, COF-18 Å, and HHTP-DPB COF) having similar topologies with different organic linkers. To the best of our knowledge, although many theoretical studies on hydrogen storage of COFs have been reported, no studies have been done for the molecular hydrogen storage and spiltover hydrogen storage on these five COFs. Therefore, the following points are investigated in this study. Firstly, the adsorption properties of H_2 on COFs are investigated using the GCMC simulations in different conditions. The effects of structural and surface properties on the hydrogen storage capacity are considered. Then the chemisorptions of the spiltover hydrogen atom on these five COFs are studied using the DFT method. Their saturation hydrogen storage densities are predicted by considering all possible adsorption sites.

2. Models and computational methods

The atomic positions of 2D COFs (PPy-COF, TP-COF, BTP-COF, COF-18 Å, and HHTP-DPB COF) studied in this paper are taken from experimental X-ray diffraction (XRD) data.[27–31] All of these five COFs are two-dimensional (2D) structures having pores only in the z direction. The pore sizes of PPy-COF, TP-COF, BTP-COF, COF-18 Å, and HHTP-DPB COF are 1.73, 3.20, 4.0, 1.8, and 4.7 nm, respectively. They have similar topologies with different organic linkers. The structural characteristics of these materials are summarized in Table 1.

Table 1. The structural characteristics of various 2D COFs.

Material	Building unit(s)	Space group	BET surface area/(m^2/g)	Lattice parameters/Å	Pore diameter/nm	Pore volume/(cm^3/g)	Ref.
PPy-COF	PDBA	$P6/mmm$	923	$a = b = 22.16$ $c = 3.426$	1.73		[27]
TP-COF	PDBA+HHTP	$P6/mmm$	868	$a = b = 37.54$ $c = 3.38$	3.20	0.7907	[28]
BTP-COF	BTPA+THDMA	$P6/mmm$	2000	$a = b = 43.65$ $c = 3.52$	4.0	1.63	[29]
COF-18Å	BTBA+THB	$P6/mmm$	1260	$a = b = 20.81$ $c = 3.46$	1.8	0.29	[30]
HHTP-DPB	HHTP+DPB	$P6/mmm$	2640	$a = b = 46.91$ $c = 3.37$	4.7		[31]

2.1. The GCMC simulations

The adsorption properties of H_2 on COFs are simulated using the grand canonical Monte Carlo (GCMC) method as implemented in the multipurpose simulation code, Music.[32] During the GCMC simulations, the COFs' structures are treated as a rigid structure, with atom positions obtained by the XRD experimental data. A $2 \times 2 \times 2$ supercell is used for COFs frameworks. The periodic boundary conditions are ap-

plied in all three dimensions in order to simulate an infinite system. The adsorption isotherms are calculated at 298 K and 77 K throughout a wide range of pressure (from 10^{-6} bar to 100 bar) to obtain a complete picture of the adsorption properties. For each point on the isotherm, 1×10^{-6} steps and 1×10^{-7} steps were used to equilibrate the system and to sample the data, respectively. Each Monte Carlo step consists of the insertion attempt of a new molecule, deletion attempt of an existing molecule, and translation or rotation of an existing molecule. Each possible attempt is randomly chosen with equal probability.

For a system consisting of COFs and H_2 molecules, the total energy includes van der Waals (VDW) interaction and long-range electrostatic interaction. The VDW interaction is described using Lennard–Jones (LJ) potential, and the long-range electrostatic interaction is described using Ewald summation method. The potential parameters for the framework atoms in COFs are taken from the Dreiding force field.[33] The Dreiding force field has been widely used to study the adsorption of gases in nanoporous materials.[34–38] A cut-off of 18.5 Å is used to the LJ potentials.

The isosteric heat Q_{st} of adsorption is defined as follows:[39]

$$Q_{\mathrm{st}} = RT - \left(\frac{\partial\langle \upsilon\rangle}{\partial\langle N\rangle}\right)_T,$$

where R is the ideal gas constant, T is the temperature, $\langle \upsilon\rangle$ is the average potential energy of the adsorbed phase, and $\langle N\rangle$ is the average number of molecules in the adsorbed phase.

2.2. The DFT calculations

Because of the large sizes of unit cells of COFs, the cluster models are used to represent the building units of COFs. Figure 1 shows the cluster models representing the 1, 3, 5-benzenetriboronic acid (BTBA), the 1, 3, 5-benzenetris (4-phenylboronic acid) (BTPA), the 2, 3, 6, 7, 10, 11-hexahydroxytriphenylene (HHTP), the 4, 4′-diphenylbutadiynebis (boronic acid) (DPB), the pyrene-2, 7-diboronic acid (PDBA), the 1, 3, 5-Tris (trimethylsilyl)-benzene (THB), and the polyol 2, 3, 6, 7-tetrahydroxy-9, 10-dimethyl-anthracene (THDMA), respectively. All the terminations are saturated with hydrogen atoms for these cleaved clusters, which are frozen to retain the constraint originating from the crystal lattices.

We perform the DFT calculations by using the CASTEP code on a basis of plane waves and supercell approaches.[40] The generalized gradient approximation (GGA) with PW91 form[41] is used to describe exchange and correlation interaction. An energy cutoff of 550 eV and Γ point for sampling the Brillouin zone are used to optimize the geometric structure and compute the chemisorption energy in the present paper. The convergence values for the energy and the force are set to be 10^{-4} eV and 0.03 eV·Å^{-1}, respectively. To avoid interactions between adjacent periodic images, the clusters under investigation are surrounded by 20 Å of vacuum space along the x, y, and z directions. All DFT calculations are performed using periodic boundary conditions.

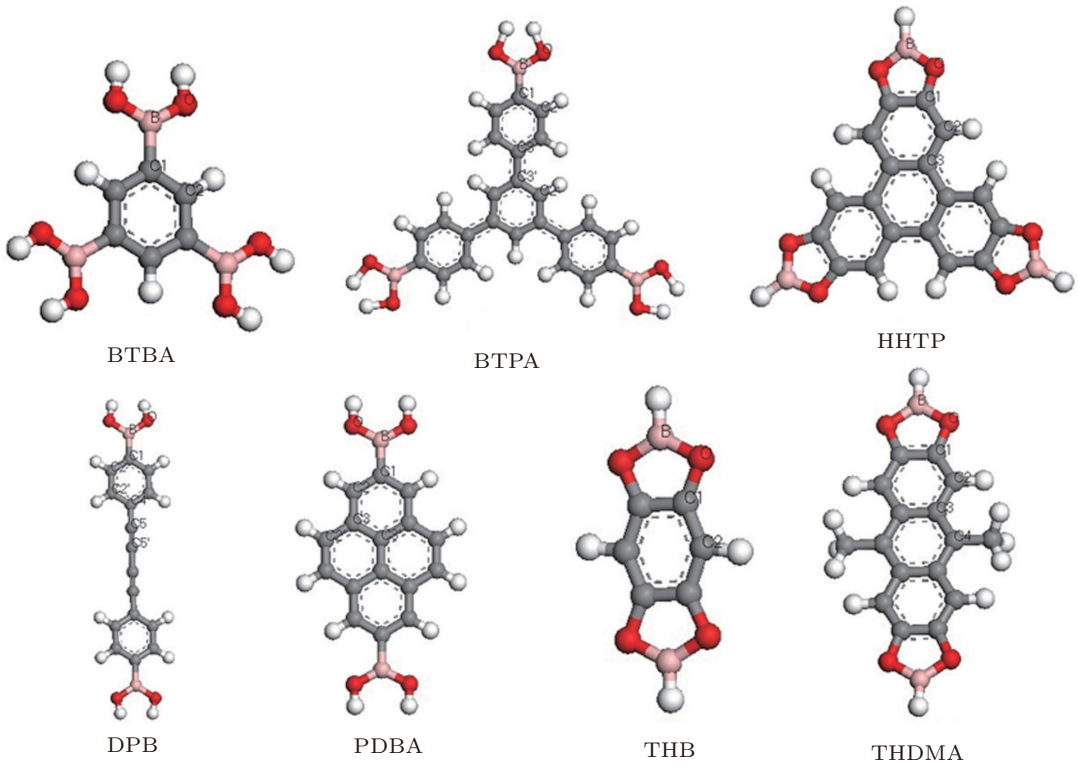


Fig. 1. (color online) Optimized structures of cluster models to represent the building units of PPy-COF, TP-COF, BTP-COF, COF-18 Å, and HHTP-DPB COF. The atomic H adsorption sites are marked in the figure.

3. Results and discussion

3.1. Adsorption of H_2 molecules on COFs

The choice of force field is crucial for an accurate description of framework atoms. In order to validate the accuracy of the simulation method used in this study, the computed adsorption isotherm of H_2 in MOF-5 at 298 K is compared with the experimental data measured by Yaghi *et al*[42] in Fig. 2. It can be seen that the simulated results are in good agreement with the experimental measurements when pressures are lower than 50 bar, and overestimate the hydrogen uptake slightly at higher pressures with a maximum deviation of 0.094 wt% at 100 bar. The disagreement between theoretical and experimental results may be attributed to several reasons, for instance, the real material has nanoporous defects and inaccessible pores due to solvent molecules left in the pore or fluid cluster formations that may stop the incoming molecules from entering the pore, while the GCMC simulations are carried out in perfect crystals. Such disagreement is also often mentioned in the literature.[43,44] Therefore, our simulated results indicate that the Dreiding force field and the GCMC program used in this study are appropriate to describe the H_2 adsorption properties of nanoporous materials like MOFs and COFs. Note that this paper will emphasize the trends in the physisorption uptakes more than the actual values themselves. These results at uniform levels may compare with the capacity of hydrogen storage on these COFs and provide some insights to help understand experimental findings.

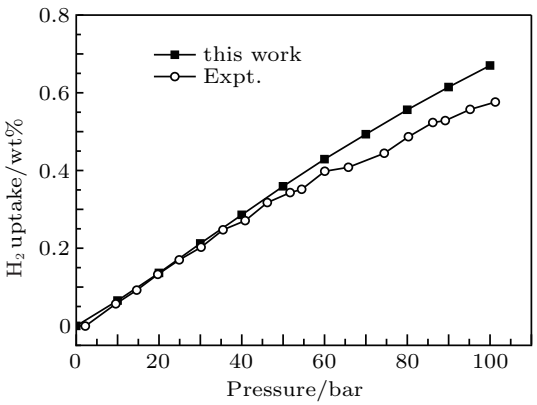


Fig. 2. Simulated and measured adsorption isotherms of H_2 in MOF-5 at 298 K. The experimental values are cited from Ref. [42].

The adsorption isotherms of H_2 in 2D COFs (PPy-COF, TP-COF, BTP-COF, COF-18 Å, and HHTP-DPB COF) at 298 K and 77 K in a broad range of pressure (from 10^{-6} bar to 100 bar) are predicted using the GCMC method, and the obtained results are shown in Fig. 3. It can be seen that HHTP-DPB COF possesses the best performance, followed by BTP-COF, TP-COF, COF-18 Å, and PPy-COF. Their H_2 uptakes reach 1.53 wt% and 4.65 wt%, 1.15 wt% and 3.53 wt%, 0.58 wt% and 1.84 wt%, 0.36 wt% and 1.20 wt%, 0.34 wt%

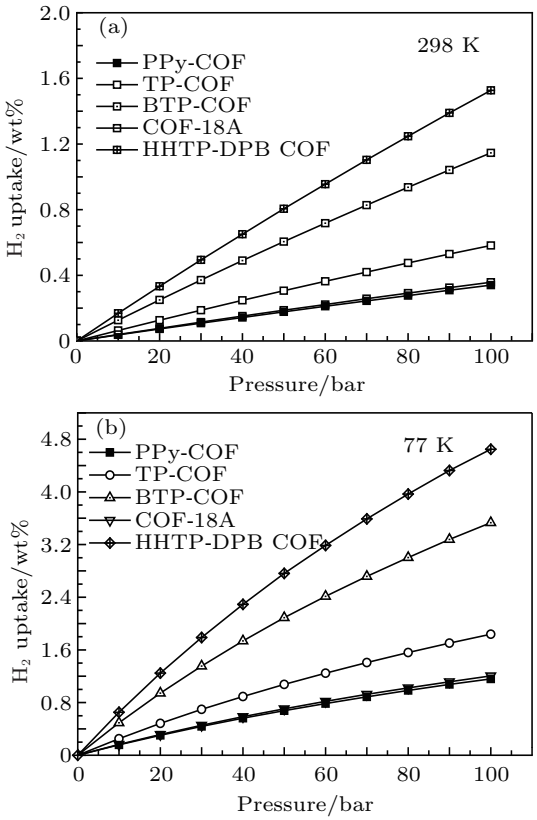


Fig. 3. Simulated adsorption isotherms of H_2 for 2D COFs at 298 K (a) and 77 K (b), respectively.

and 1.16 wt% at 298 K and 77 K at a pressure of 100 bar, respectively, which are too low to meet the uptake target set by US-DOE and enable practical applications. This is attributed to the very weak VDW interactions between H_2 and COFs, which will be confirmed by further discussion of the isosteric heat of adsorption in COFs subsequently. Next, we examine the hydrogen uptakes at 100 bar as a function of BET surface area and pore size, respectively, which are shown in Fig. 4. It can be seen that the H_2 uptake increases with the increase of surface area (except TP-COF) and pore size. Therefore, increasing surface area and pore size is a good strategy for improving the hydrogen storage capacity of 2D COFs.

In addition to surface area and pore size, adsorption enthalpy is also an important parameter to evaluate the adsorption performance of a porous material. The variations of isosteric heat of adsorption with the pressure for the total uptake of H_2 in COFs at 298 K are plotted in Fig. 5. It can be seen from this figure that the isosteric heats of H_2 are within a range of 2.38 kJ/mol–2.45 kJ/mol, thus we may conclude that the H_2 molecules interact with the COF framework through weak VDW interaction. The isosteric heat of adsorption, which gradually decreases with the increase of pressure (i.e., adsorption amount), indicates that the gas-COF interaction decreases with the increase of the amount of molecular hydrogen due to the stronger binding sites being occupied first.[45] It can also be seen that the isosteric heat of adsorption in HHTP-DPB

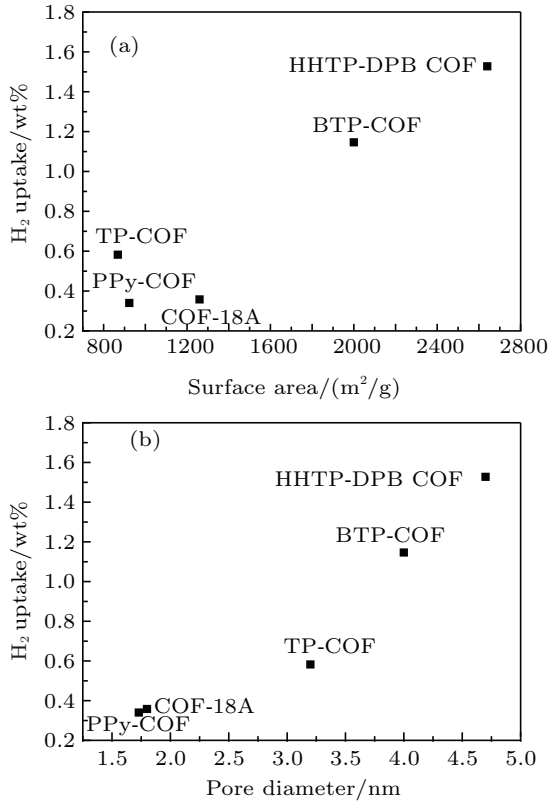


Fig. 4. Adsorption uptake of H_2 as a function of BET surface area (a) and pore diameter (b) for 2D COFs at 298 K and 100 bar.

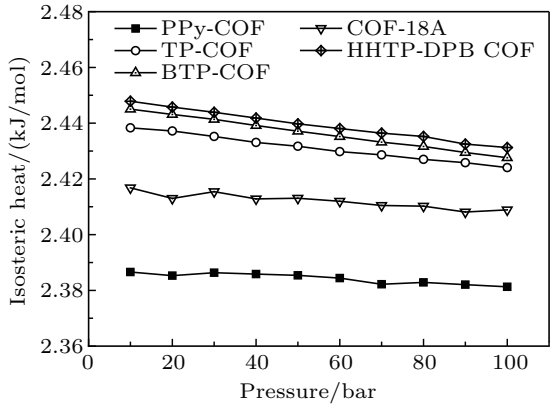


Fig. 5. Variations of isosteric heat of adsorption of H_2 with pressure for 2D COFs at 298 K.

COF is highest, followed by BTP-COF, TP-COF, COF-18 Å, and PPy-COF. This order is consistent with the adsorbed amount. Therefore, isosteric heat of adsorption as well as surface area and pore size is also an important factor for determining the uptake of H_2.

3.2. Adsorption of H atom on COFs by spillover

As is shown in Fig. 3, among these five COF materials, the H_2 uptakes are still poor at room temperature with the highest value being 1.53 wt% for HHTP-DPB COF at 100 bar. Therefore, the physisorption of molecular hydrogen on porous materials through weak VDW interaction is insufficient for storage applications. Hydrogen spillover has been demonstrated as an effective approach to the enhancement of the hydrogen storage capacity in porous materials at ambient temperature.[20–24] Thus we study the chemisorptions of spiltover hydrogen atoms on these five COFs represented by the cluster models (Fig. 1) using the DFT method. For these cluster models, we consider all possible adsorption sites, which are labeled in Fig. 1. All possible adsorption sites are B sites, O sites, and C sites, where the B site is on the top of B atom, the O site is on the top of O atom, and the C sites can be divided into five categories based on their adjacent atoms: (i) the C atom adjacent to B or O atom, labeled as C1 site, (ii) the C atom adjacent to one H atom and two sp^2 hybridized C atoms, labeled as C2 site, (iii) the C atom adjacent to three sp^2 hybridized C atoms, labeled as C3 site, (iv) the C atom adjacent to two sp^2 hybridized C atoms and one sp^3 hybridized C atom, labeled as C4 site, (v) the C atom adjacent to one sp^3 hybridized C atom and one sp hybridized C atom, labeled as C5 site.

Table 2. Values of adsorption energy (ΔE_H) of hydrogen atom and the bond length (d_{C-H}) of C–H at different adsorption sites.

Cluster	Sites	ΔE_H/eV	d_{C-H}/Å	Cluster	Sites	ΔE_H/eV	d_{C-H}/Å
BTBA	C1	0.849	1.135	THDMA	O	−1.05	0.990
	C2	1.364	1.116	BTPA	C1	1.039	1.129
HHTP	C1	0.893	1.125		C2	1.139	1.113
	C2	1.663	1.113		C3	0.777	1.124
	C3	0.794	1.128		C2′	1.762	1.111
PDBA	C1	0.826	1.135		C3′	0.587	1.123
	C2	1.718	1.110	DPB	C1	1.496	1.131
	C3	0.496	1.135		C2	1.478	1.107
	C2′	1.347	1.116		C2′	1.513	1.112
	C3′	0.619	1.130		C4	1.275	1.125
THDMA	C1	1.018	1.116		C5	2.007	1.108
	C2	1.635	1.109		C5′	1.759	1.110
	C3	0.403	1.135	THB	C1	0.842	1.119
	C4	1.549	1.111		C2	1.219	1.115

The binding energies of an H atom placed in all possible adsorption sites of the building units are calculated using the DFT theory. The binding energy (BE) is defined as $\Delta E_H = (E_{cluster} + E_H) - E_{cluster+H}$. The studied results show that for the O sites of HHTP and THB clusters, even if the H atom is initially placed at the O site, it would converge to its neighboring B site after structure relaxation. This indicates that the O site is unable to bind the H atom. For the O site of THDMA cluster, the binding energy is a negative value of −1.05 eV with an O–H bond length of 0.990 Å (shown in Table 2), which demonstrates that the O–H bond is unstable under normal conditions. Therefore, the O site is not a suitable chemisorption site for the H atom. Next, we examine the B sites of BTBA, BTPA, PDBA, and DPB clusters. We find that the H atom placed at the B site initially can move to the neighboring C site and form C–H bond with the bond lengths

of 1.141 Å for BTBA, 1.143 Å for BTPA, 1.136 Å for PDBA, and 1.132 Å for DPB, which indicates that the B site is also an inappropriate adsorption site for the spilt hydrogen atom.

For C1, C3, and C4 sites, the H atoms can be directly adsorbed on their tops with the C–H bond and neighboring C–C bonds representing sp^3 states. The values of binding energy ΔE_{H} of the H atom and the C–H bond length $d_{\mathrm{C-H}}$ at different sites are listed in Table 2. It can be seen that the ΔE_{H} values on C1, C3, and C4 sites are in a range of 0.403 eV–1.549 eV with the $d_{\mathrm{C-H}}$ being between 1.111 Å and 1.135 Å. For the C2 site, one H atom is situated symmetrically to the pre-existing H atom. The ΔE_{H} values are in a range of 1.139 eV–1.762 eV, which are larger than those of C1, C3, and C4 sites with the same cluster, yet the $d_{\mathrm{C-H}}$ between 1.109 Å and 1.116 Å are smaller than those of C1, C3, and C4 sites accordingly. This indicates that the C2 sites are more stable adsorption sites than C1, C3, and C4 sites.

For the C5 site, one H atom and two H atoms are initially placed on the top of it, respectively. The results show that the average binding energies of two H atoms are only 0.501 eV and 0.212 eV for C5 and C5′ sites, respectively, which are much lower than those of one H atom (2.007 eV and 1.759 eV). We can conclude that only one H atom can bind to the C5 site stably.

Based on the above discussion, we may obtain the following conclusions: each C site may adsorb one H atom, while the B and the O sites are inappropriate to adsorb the H atom thermodynamically. This is consistent with the work of Ganz *et al.*[18,19] Therefore, the saturated cluster models representing these five COFs at a saturated level are constructed by placing one H atom on each C site of each cluster, which are shown in Fig. 6. The average binding energy and the saturation storage density of hydrogen are calculated, and the results are shown in Tables 3 and 4, respectively. The average binding energy is defined as $\overline{\Delta E_{\mathrm{H}}} = [(E_{\mathrm{cluster}} + NE_{\mathrm{H}}) - E_{(\mathrm{cluster+NH})}]/N$. It can be seen from Table 3 that the $\overline{\Delta E_{\mathrm{H}}}$ values are in a range of 2.676 eV–10.593 eV, which are larger than the binding energy (2.26 eV) of the H_2 molecule for the spillover process to proceed smoothly and reversibly.[19] The hydrogen storage on amorphous carbon or graphite, or grapheme,[44] will be difficult at room temperature due to insufficient binding energy.

We can see that from Table 4 the saturation hydrogen storage density of 6.17 wt% for BTP-COF is largest, followed by 6.11 wt% for HHTP-DPB COF, and TP-COF, 5.99 wt% for PPy-COF, and 4.79 wt% for COF-18 Å. The saturation hydrogen storage densities of these COFs are much larger

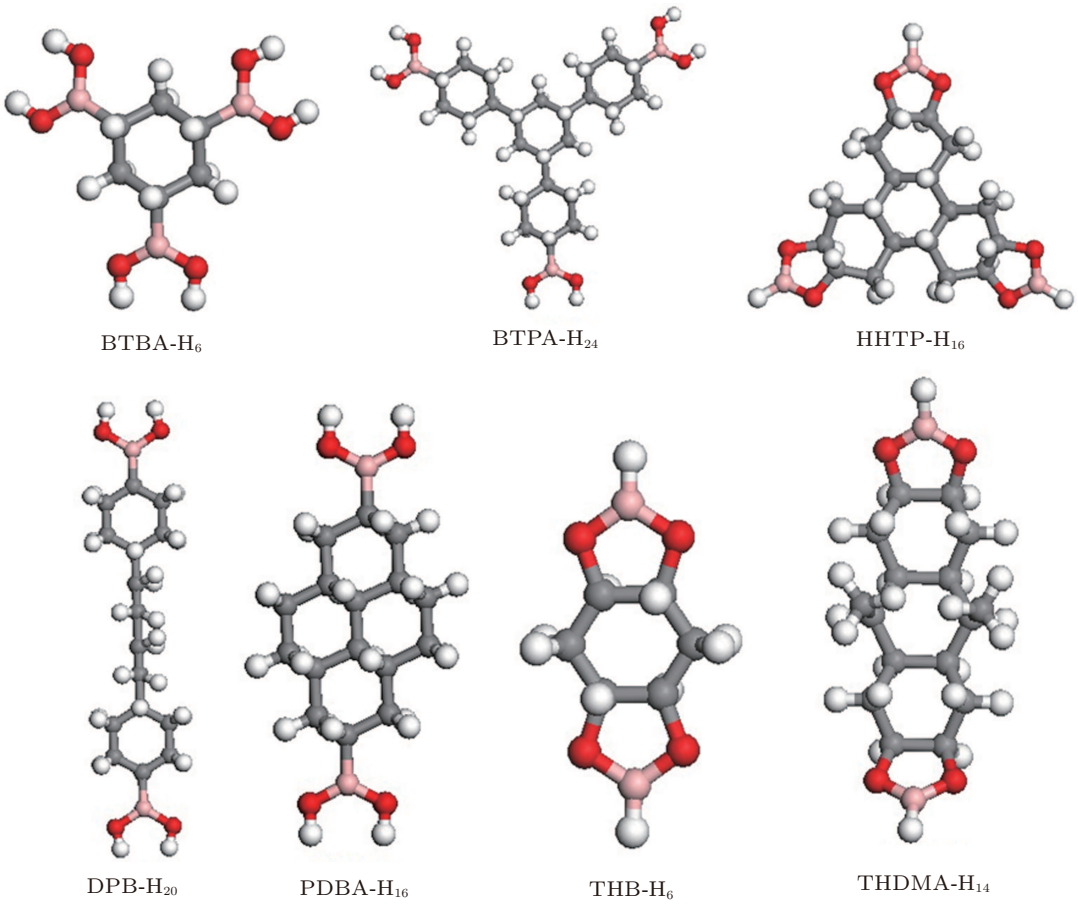


Fig. 6. (color online) Optimized structures of hydrogenated cluster models of PPy-COF, TP-COF, BTP-COF, COF-18 Å, and HHTP-DPB COF at a saturated level.

Table 3. Values of average adsorption energy ($\overline{\Delta E_{\rm H}}$) of hydrogen atoms adsorbed on different linkers at a saturated level.

Cluster	$\overline{\Delta E_{\rm H}}$/eV
BTBA	10.593
HHTP	4.909
PDBA	2.719
BTPA	2.771
THDMA	2.714
THB	2.676
DPB	2.769

Table 4. Predicted saturation storage densities of hydrogen by spillover for various 2D COFs.

Material	Formula unit	Number of H per formula unit	Saturation storage density/wt%
PPy-COF	$C_{48}H_{24}B_6O_6$	48	5.99
TP-COF	$C_{84}H_{36}O_{12}B_6$	84	6.11
BTP-COF	$C_{96}H_{60}B_6O_{12}$	96	6.17
COF-18 Å	$C_{34}H_{16}B_6O_{12}$	34	4.79
HHTP-DPB	$C_{84}H_{36}B_6O_{12}$	84	6.11

than the physisorption amount of H_2 obtained using GCMC method at 298 K and 100 bar. This suggests that the hydrogen uptake may be significantly enhanced with these materials by spillover. It can also be seen that almost all of the saturation storage densities of these COFs (except COF-18 Å) are higher than those of most MOFs reported by Suri *et al.*[19] and are close to or exceed the 2010 DOE target of 6 wt% for hydrogen storage. This indicates that 2D COFs studied in this paper are suitable hydrogen storage media by spillover.

4. Conclusions

In this work, molecular hydrogen and spiltover hydrogen storage on five 2D COFs (PPy-COF, BTP-COF, TP-COF, COF-18 Å, and HHTP-DPB COF) are investigated using the GCMC simulations and the DFT method, respectively. Some important physical quantities under different temperatures and pressures, such as adsorption isotherm, adsorption amount, and isosteric heat of adsorption are obtained by the GCMC simulations. The results show that HHTP-DPB COF has the best performance for hydrogen storage, followed by BTP-COF, TP-COF, COF-18 Å, and PPy-COF. The hydrogen uptake at 100 bar as a function of BET surface area and pore size indicates that the H_2 uptake increases with the increases of surface area (except TP-COF) and pore size. The computed isosteric heats of H_2 in COFs at 298 K indicate that the H_2 molecules interact with the COF framework through weak VDW interaction.

The DFT study on the spiltover hydrogen storage shows that each C site may adsorb one H atom, while the B and the O sites are unable to adsorb an H atom thermodynamically. The saturation cluster models are constructed based on this conclusion. The computed large average binding energy indicates that the spillover process may proceed smoothly and reversibly. The obtained saturation hydrogen storage densities in a range of 4.79 wt%–6.17 wt% are close to or exceed the 2010 DOE target for hydrogen storage, which suggests that the hydrogen storage capacities of these COF materials may be dramatically enhanced by spillover. We can conclude that 2D COFs each have a good potential to be suitable hydrogen storage media by spillover. Therefore, more attempts should be made at synthesizing new COFs and studying their hydrogen storage properties by spillover in expectation of finding new materials with even higher storage capacities.

References

[1] Satyapal S, Petrovic J, Read C, Thomas G and Ordaz G 2007 *Cat. Today* **120** 246
[2] Côté A P, Benin A I, Ockwig N W, O'Keeffe M, Matzger A J and Yaghi O M 2005 *Science* **310** 1166
[3] Hunt J R, Doonan C J, LeVangie J D, Côté A P and Yaghi O M 2008 *J. Am. Chem. Soc.* **130** 11872
[4] Tilford R W, Mugavero III S J, Pellechia P J and Lavigne J J 2008 *Adv. Mater.* **20** 2741
[5] Wan S, Guo J, Kim J, Ihee H and Jiang D 2008 *Angew. Chem.* **120** 8958
[6] Spitler E L and Dichtel W R 2010 *Nat. Chem.* **2** 672
[7] Spitler E, Colson J W, Uribe-Romo F J, Woll A R, Saldivar M R G A and Dichtel W R 2012 *Angew. Chem.* **124** 1
[8] Klontzas E, Tylianakis E and Froudakis G E 2008 *J. Phys. Chem. C* **112** 9095
[9] Furukawa H and Yaghi O M 2009 *J. Am. Chem. Soc.* **131** 8875
[10] Assfour B and Seifert G 2010 *Micropor. Mesopor. Mat.* **133** 59
[11] Wong-Foy A G, Matzger A J and Yaghi O M 2006 *J. Am. Chem. Soc.* **128** 3494
[12] Lan J H, Cao D P and Wang W C 2010 *J. Phys. Chem. C* **114** 3108
[13] Wu M M, Wang Q, Sun Q, Jena P and Kawazoe Y 2010 *J. Chem. Phys.* **133** 154706
[14] Zou X L, Zhou G, Duan W H, Choi K and Ihm J 2010 *J. Phys. Chem. C* **114** 13402
[15] Yang Z L and Cao D P 2012 *J. Phys. Chem. C* **116** 12591
[16] Mendoza-Cortes J L, Han S and Goddard III W A 2012 *J. Phys. Chem. A* **116** 1621
[17] Guo J H, Zhang H, Liu Z P and Cheng X L 2012 *J. Phys. Chem. C* **116** 15908
[18] Suri M, Dornfeld M and Ganz E 2009 *J. Chem. Phys.* **131** 174703-1
[19] Ganz E and Dornfeld M 2012 *J. Phys. Chem. C* **116** 3661
[20] Li Y W and Yang R T 2008 *AIChE* **54** 269
[21] Lachawiec A J Jr, Qi G and Yang R T 2005 *Langmuir* **21** 11418
[22] Jiménez V, Ramírez-Lucas A, Sánchez P and Valverde J L 2012 *Int. J. Hydrog. Energ.* **37** 4144
[23] Lachawiec A J Jr and Yang R T 2008 *Langmuir* **24** 6159
[24] Li Y W and Yang R T 2006 *J. Am. Chem. Soc.* **128** 8136
[25] Kim H S, Lee H, Han K S, Kim J H, Song M S, Park M S, Lee J Y and Kang J U 2005 *J. Phys. Chem. B* **109** 8983
[26] Lee K, Kim Y H, Sun Y Y, West D, Zhao Y F, Chen Z F and Zhang S B 2010 *Phys. Rev. Lett.* **104** 236101
[27] Wan S, Guo J, Kim J, Ihee H and Jiang D L 2009 *Angew. Chem. Int. Ed.* **48** 5439
[28] Wan S, Guo J, Kim J, Ihee H and Jiang D L 2008 *Angew. Chem.* **120** 8958
[29] Dogru M, Sonnauer A, Gavryushin A, Knochel P and Bein T 2011 *Chem. Commun.* **47** 1707
[30] Tilford R W, Gemmill W R, zur Loye H and Lavigne J J 2006 *Chem. Mater.* **18** 5296
[31] Spitler E L, Koo B T, Novotney J L, Colson J W, Uribe-Romo F J, Gutierrez G D, Clancy P and Dichte l W R 2011 *J. Am. Chem. Soc.* **133** 19416
[32] Gupta A, Chempath S, Sanborn M J, Clark L A and Snurr R Q 2003 *Mol. Simul.* **29** 29

[33] Mayo S L, Olafson B D and Goddard W A 1990 *J. Phys. Chem.* **94** 8897
[34] Sarkisov L, Duren T and Snurr R Q 2004 *Mol. Phys.* **102** 211
[35] Garberoglio G, Skoulidas A I and Johnson J K 2005 *J. Phys. Chem. B* **109** 13094
[36] Duren T, Sarkisov L, Yaghi O M and Snurr R Q 2004 *Langmuir* **20** 2683
[37] Liu X Y, Wang C Y, Tang Y J, Sun W G and Wu W D 2010 *Chin. Phys. B* **19** 036103
[38] Liu X Y, Wang C Y, Tang Y J, Sun W G, Wu W D, Zhang H Q, Liu M, Yuan L and Xu J J 2009 *Acta Phys. Sin.* **58** 1126 (in Chinese)
[39] Snurr R Q, Bell A T and Theodorou D N 1993 *J. Phys. Chem.* **97** 13742
[40] Clark S J, Segall M D, Pickard C J, Hasnip P J, Probert M J, Refson K and Payne M C 2005 *Zeitschrift für Kristallographie* **220** 567
[41] Perdew J P and Wang Y 1992 *Phys. Rev. B* **45** 13244
[42] Kaye S S, Dailly A, Yaghi O M and Long J R 2007 *J. Am. Chem. Soc.* **129** 14176
[43] Klontzas E, Tylianakis E and Froudakis G E 2008 *J. Phys. Chem. C* **112** 9095
[44] Garberoglio G, Skoulidas A I and Johnson J K 2005 *J. Phys. Chem. B* **109** 13094
[45] Llewellyn P L and Maurin G 2005 *C. R. Chimie* **8** 283
[46] Psofogiannakis G and Froudakis G 2009 *J. Phys. Chem. C* **113** 14908